Implementation of highly sensitive small extracellular vesicle (sEV) quantification method in the identification of novel sEV production modulators and the evaluation of sEV pharmacokinetics

(要約版)

2021

Aki Yamamoto

Table of Contents

Preface

Small extracellular vesicles (sEVs) are a heterogenous group of lipid-bilayer enclosed nanovesicles that are secreted by majority of cell types into nearly all biological fluids including blood, saliva, and urine[1–3]. They play an integral part in cell-cell communication by delivering their molecular cargoes to the recipient cells to modulate diverse biological and pathological processes in the body[4,5]. Quantification of sEVs is a key aspect of sEV research as the amount of sEVs have been reported to alter during disease states and contribute significantly to its progression.

Various physical and biochemical methods for sEV quantification have been reported in the literature thus far[6,7]. One of the most popular methods of sEV quantification is nanoparticle tracking analysis, which quantifies not only the concentration, but also the size distributions of the isolated sEVs[8]. Additionally, colorimetric protein assays are commonly used to quantify the total protein content of sEVs. Tunable resistive pulse sensing is another technique that has been adapted to quantify sEVs by detecting the changes in electrical current, which ultimately reflects the volume of nanoparticle passing the detector[8]. In addition to physical sEV quantification methods, biochemical methods, such as immunoblotting, ELISA, and flow cytometry are also commonly utilized to quantify specific subpopulation of sEVs from a biological or clinical sample[9–12].

However, majority of these quantification methods are limited to measuring highly purified sEV samples. In fact, most of the physical methods for sEV quantification are used in combination with ultracentrifugation or size exclusion chromatography-based sEV isolation methods to eliminate protein contaminations as it could potentially influence the quantification assay. These isolation methods are very time-consuming, thus does not allow for measurement of multiple samples simultaneously[13]. Biochemical methods also require time-consuming pre-treatment of the target samples and optimization of the measuring condition prior to use.

Therefore, in this thesis, a convenient, highly sensitive sEV quantification assay was developed utilizing *Gaussia* luciferase (gLuc) reporter protein fused to sEV marker proteins to quantify the sEV levels based on the luciferase activity of the sample. Utilizing this quantification method, in chapter I, high throughput screening was performed to identify novel small molecule compounds that can regulate sEV production. To further understand the sEV production and its *in vivo* fates during disease pathogenesis, in chapter II, a variation of the gLuc fusion proteins were utilized to elucidate the mechanism behind elevated plasma sEV levels observed during cancer pathogenesis. Finally, in chapter III, another gLuc fusion protein was utilized to investigate the roles of surface glycans in sEV pharmacokinetics.

Chapter I Development of a highly sensitive sEV quantification method and the identification of novel sEV modulators via high throughput screening

The nature and abundance of the sEVs are dependent on the types of sEV-producing cells, as well as the physiological or pathological state of the parent cells, and influence the biological functions of sEVs. Normally, sEVs maintain homeostasis and regulate immune responses in the body[14,15]; however, sEVs also plays a role in disease onset and progression. For example, in cancer, it is well-known that tumor cells secrete sEVs and that these circulating sEVs facilitate disease progression by promoting tumorigenesis, immune escape, and metastasis[16].

Owing to its role in disease progression, the identification of small molecule compounds that regulate sEV production is becoming increasingly popular as a novel therapeutic strategy. In addition, such molecules are also beneficial as an experimental tool to identify certain sEV functions during biological or pathological processes. Furthermore, small molecules can be utilized to further our understanding of molecular machineries involved in the sEV biogenesis pathway.

Investigation of the sEV biogenesis pathway has led to reports of various agents that modulate sEV biogenesis/release in the recent years[17–22]. One of the main setbacks for identifying potent sEV production modulators was the lack of a high throughput system for quantifying sEV production; generally, sEV quantification require time-consuming purification steps, which significantly decreased throughput. However, the development of a cell-based high throughput assay system utilizing CD63-GFP has allowed quantitative high throughput screening (HTS) of existing drug libraries to identify potent modulators of sEV production[23,24]. Nonetheless, these assay systems relied on the changes in intracellular CD63-GFP signals to identify potent activators and inhibitors of sEV production, thus did not directly measure the sEV production.

In this study, a rapid, highly sensitive sEV quantification method utilizing *Gaussia* luciferase (gLuc) reporter protein was developed for HTS. gLuc protein fused to sEV marker proteins—CD63 and CD82—were utilized to label the inner spaces of the sEV membrane to quantify the sEV production based on the chemiluminescence of the cell supernatant. Because the gLuc fusion proteins could also be present as soluble proteins or as parts of cell debris in the supernatant, pre-treatment conditions by centrifugation (to eliminate cells/cell debris) and proteinase K (ProK) treatment (to eliminate soluble proteins) were evaluated. After confirming the validity of the developed assay, 480 compounds from our in-house chemical libraries were screened, and compound A and compound B were identified as potent sEV production inducers and inhibitors, respectively. Compound-treated conditioned medium hardly impacted the chemiluminescence emitted by the gLuc enzyme. Contrastingly, significant changes in gLuc activity of the culture medium of cells treated with the 2 compounds were observed in a dose-dependent manner, with relatively low cellular toxicity at the investigated doses. Changes in sEV production by the 2 compounds were confirmed by isolating the sEVs from compound-treated cells via ultracentrifugation and measuring the total protein yield. Further investigation of compound B suggested the role of autophagy induction and inhibition of sEV release as the potential mechanism for its inhibitory effect on sEV production.

Thus, in chapter I, a convenient, highly sensitive chemiluminescent-based sEV quantification assay was successfully developed. Utilizing the developed assay, sEV production modulators were investigated via HTS and two compounds were successfully identified as potent inhibitor or inducer of sEV production. The identified compounds from the screen will be a useful tool in wide range of sEV research and, potentially, in sEV-based therapeutic treatment.

Chapter II Pharmacokinetic approach for the elucidation of elevated plasma sEV concentration during cancer pathogenesis

Because the rate of sEV production and cargo contents depends on the state of the producing cells, the quality and quantity of sEVs can change during disease pathogenesis. Total plasma sEV levels have been reported to increase significantly during cancer and correlate with disease progression[25–28]. Therefore, investigation of sEVs as potential biomarkers for diagnosis and disease progression have advanced rapidly[27,29]. Additionally, novel cancer therapeutic strategies targeting circulating tumor-derived plasma sEVs either by extracorporeal hemofiltration or antibodies have been studied as well[30,31].

Further understanding of the mechanism by which plasma sEV concentrations are elevated during cancer is crucial in developing novel therapeutic approaches. However, this remains a challenge due to the technical difficulties in tracking and properly evaluating the sEV production rate *in vivo*. Quantification of sEV production from cell culture-derived sEVs have been proposed using CD63-pHluorin or CD63-nanoLuc-expressing cell line[32–34]. Although these methodologies can be advantageous for quantifying sEV secretion with high sensitivity *in vitro*, its use *in vivo* have been limited to biodistribution studies. More recently, utilization of Cre/LoxP system in tracking endogenous sEVs have been reported by incorporating tissue-specific promoters to selectively express reporter proteins for sEV labeling in transgenic mice upon tamoxifen induction, which may provide beneficial information regarding sEV secretion *in vivo* in the future[35–37].

Previously, our laboratory has developed a more practical, yet highly sensitive sEV labeling method utilizing a fusion protein consisting of gLuc and lactadherin (LA) (gLuc-LA) to track the *in vivo* fate of mouse plasma-derived sEVs (MP-sEVs). Physiochemically intact sEVs were isolated via size exclusion chromatography (SEC), labeled with gLuc-LA, and intravenously administered to the tail-vein of the mice to estimate the clearance rate and the theoretical secretion rate of MP-sEVs[38]. By implementing this labeling method, plasma sEV dynamics in healthy and diseased-states could be evaluated to elucidate the mechanism of elevated plasma sEV concentration during disease pathogenesis.

In this study, a pharmacokinetic (PK) approach was taken to understand the MP-sEV dynamics during tumor pathology using tumor-bearing mice as a model. Isolation of MP-sEVs from B16BL6-tumor bearing mice showed 3-fold increase in MP-sEV protein yield compared to healthy (NT) mice. The zeta potential, morphology, size, and protein profile of the isolated MP-sEVs were comparable regardless of the health state of the mice.

Since the steady-state concentration of MP-sEVs is maintained by a balance between the rate of elimination (k_{el}) and rate of secretion (k_0), the elevated plasma sEV concentration was either due to decreased k_{el} or increased k_0. To determine the effect of tumor pathology on MP-sEV clearance, gLuc-LA labeled MP-sEVs isolated from NT and tumor-bearing mice were intravenously administered into either of the two mice. Results showed that regardless of the health state of the mice from which the sEVs were derived from, MP-sEVs disappeared immediately from the blood circulation in both healthy and tumor-bearing mice. This suggested that the elevated plasma MP-sEV levels likely resulted from an increased sEV secretion. However, gLuc activity of the MP-sEVs isolated from the plasma of B16BL6-CD63-bearing mice was below the limit of detection. This suggested very little tumor cell-derived sEVs in the total MP-sEVs and cells other than tumor cells contributed to the increased sEV production during tumor pathology.

Thus, in chapter II, it was determined that the elevated sEV concentration during tumor pathology was due to increased sEV production rate; however, tumor cell-derived sEVs had very little contribution to the overall MP-sEV levels, thus sEV productions was likely increased in cells other than tumor cells in tumor pathology. These findings will provide useful insight into the clarification of the roles of sEVs in tumor progression and into the development of sEV-targeting cancer therapy.

Chapter III Determination of the effect of surface glycans in sEV pharmacokinetics

III-1 Introduction

sEV surface glycans are one of the major constituents of sEVs alongside proteins and membrane lipid that play a role in many key processes including sEV biogenesis, cargo recruitment, cellular recognition, and cellular uptake[39–42]. Additionally, sEV derived from cancer cells has been reported to show enrichment of specific glycans on its membrane surface. For instance, ovarian cancer cell-derived sEVs have increased presence of specific mannose- and sialic acid-containing glycoproteins on its sEV surface[43], which could potentially be used as promising biomarkers for cancer diagnosis and/or prognosis.

Considering that surface glycans are located on the outermost region of the sEV surface, they may have significant impact on the sEV pharmacokinetics. However, general investigation of sEV surface glycans has been lagging behind that of surface lipids and proteins, mostly due to its structural complexity and lack of available endoglycosidases or suitable chemical methods to liberate specific glycans for analysis[44,45]. Although there have been reports on the roles of glycans in protein pharmacokinetics[46–48], information regarding the roles of surface glycans in sEV pharmacokinetics at the whole-body level remains limited. Recently the removal of O-glycans, but not N-glycans, was reported to increase the distribution of brain-metastatic breast cancer cell-derived sEVs into the lungs, suggesting an inhibitory role of O-glycans on sEV uptake *in vivo*[49]. Additionally, desialylation of sEVs has been shown to impact not only its cellular uptake *in vitro*, but also its biodistribution *in vivo*[50].

In the present study, the role of surface glycans in sEV pharmacokinetics was investigated by enzymatically removing the N- and O-glycans using Peptide-N-Glycosidase F (PNGase F) and O-glycosidase, respectively, from the sEV surface. PNGase F removes nearly all N-glycans from glycoproteins, while O-glycosidase cleaves a specific type of O-glycans—the unsubstituted GalNAc disaccharides—thus, requires the presence of neuraminidase to cleave the sialic acid residues, if present on the disaccharides[51]. B16BL6 cell-derived sEVs were labeled with the fusion protein, Gag-gLuc, to preserve the reporter protein activity after glycosidase treatment. The physicochemical properties of the isolated untreated and glycosidase-treated sEVs and its cellular uptake in peritoneal macrophages were evaluated. Then, the effect of sEV surface glycans on its pharmacokinetics was determined by intravenous tail-vein injection of the labeled sEVs into the mice.

III-2 Materials and Methods

Animals

Four-to six-week-old male ICR mice were purchased from Shimizu Laboratory Supplies. Protocols for animal experiments were approved by the Animal Experimentation Committee of the Graduate School of Pharmaceutical Sciences of Kyoto University.

Cell culture and transfection

B16BL6 murine melanoma cell line was obtained from RIKEN BioResource Center and cultured as described in previous sections. Mouse peritoneal macrophages were collected and cultured as per a previously described method with modifications[52]. Briefly, mice were stimulated with an intraperitoneal injection of 2 mL 4.05% thioglycolate medium (Nissui Co. Ltd.). Three days post-administration, mice were sacrificed and injected with 5 mL ice-cold PBS into the peritoneal cavity. After 2 min, the peritoneal lavage fluid was collected and centrifuged at 400 × *g* for 10 min to sediment the cells. Cells were washed and suspended in RPMI-1640 medium (Nissui Co. Ltd.) supplemented with 0.15% sodium bicarbonate and PSG (Nacalai Tesque Inc.), and then seeded into a 96-well plate at a density of 2.5×10^5 cells/well for cellular uptake assay.

pDNA encoding Gag-gLuc was prepared as described previously[53].

sEV isolation

Conditioned medium of Gag-gLuc transfected B16BL6 cells was collected and subjected to sequential centrifugation as described in previous sections. Subsequently, the supernatant was passed through 0.2 μm syringe filters and spun at 100,000 × *g* for 1-2 h (Hitachi Koki). The resulting sEV pellets were washed once with filtered PBS prior to deglycosylation.

For deglycosylation, PNGase F (purified from *Flavobacterium meningosepticum*) and O-glycosidase & α2-3,6,8 Neurmainidase Bundle (cloned from *Enterococcus faecalis* and *Clostridium perfringens*, respectively) were purchased from New England Biolabs (Ipswich, MA, USA). sEV pellets were treated with a medium dose of either PNGase F (1250 U), O-glycosidase (100,000 U) with neuraminidase (125 U), or a combination of the three glycosidases and incubated at 37°C for 3 h. The mixture was then washed twice by ultracentrifugation for 1 h at 100,000 ×*g* to remove excess glycosidases. The final sEV pellets were resuspended in small volumes of PBS (50-100 μL), and the protein concentrations were determined using the Quick Start Bradford protein assay (Bio-Rad). The dose for deglycosylation treatment was determined using fetuin (New England Biolabs), as described subsequently.

For fluorescent labeling, PKH67 green fluorescent cell linker kit was purchased from Sigma Aldrich. The sEV pellets were labeled with PKH67 dye prior to deglycosylation as described previously[54].

Coomassie Brilliant Blue (CBB) Staining
Fetuin was treated with either low (26 U/μg protein PNGase F; 2,080 U/μg protein O-glycosidase; 2.6 U/μg protein neuraminidase), medium (52 U/μg protein PNGase F; 4,160 U/μg protein O-glycosidase; 5.2 U/μg protein neuraminidase), or high (105 U/μg protein PNGase F; 8,400 U/μg protein O-glycosidase; 10.5 U/μg protein neuraminidase) doses of the glycosidase enzymes and incubated at 37℃ for 3 h to determine the minimum amount of enzymes required for deglycosylation. For CBB staining, the untreated and glycosidase-treated samples were reduced with 100 mM DTT at 95℃ for 3 min and subjected to 10% SDS-PAGE. After fixing the gel for 30 min, it was stained with 0.25% w/v CBB R-250 (Fujifilm) for 60 min, followed by 2-3 h of destaining until the protein bands became visible against the background of the gel matrix. The gel was visualized using LAS-3000 imaging system (Fujifilm).

Lectin blotting
sEV samples were reduced with 100 mM DTT at 95°C for 3 min and subjected to 10% SDS-PAGE. The separated proteins were then transferred to PVDF membrane (Merck Millipore Ltd.). After blocking for 30 min with Blocking One reagent (Nacalai Tesque Inc.), the membranes were incubated with biotinylated lectins diluted in PBS (1:2000 dilution; Vector Laboratories Inc., Burlingame, CA, USA) for 30 min at 25°C. Subsequently, the membranes were incubated with Vectastain ABC-HRP reagent (1:100 dilution; Vector Laboratories Inc.) for 30 min at 25°C. Following incubation, the membranes were washed with twice with 0.05% Tween 20 PBS (PBS-T), once with PBS, and then reacted with Immobilon Western Chemiluminescent HRP substrate (Merck Millipore Ltd.). Chemiluminescence was detected using LAS-3000 imaging system (Fujifilm).

Western blotting
B16BL6 cell lysates were prepared by multiple rounds of freezing and thawing, followed by centrifugation at 10,000 × *g* for 10 min. Western blotting of sEV markers (Alix, Hsp70, CD81, Calnexin) were conducted as described in previous sections. The following primary antibodies were utilized: mouse anti-AIP1 (49/AIP1) antibody (1:1000; BD Biosciences), rabbit anti-Hsp70 antibody (1:1000; Cell Signaling Technology), anti-CD81 (H-121) antibody (1:200; Santa Cruz Biotechnology), and rabbit anti-Calnexin (H-70) antibody (1:1000; Santa Cruz Biotechnology). The following HRP-conjugated secondary antibodies were utilized for detection: rabbit anti-mouse IgG antibody (1:1000; Thermo Fisher Scientific) and goat anti-rabbit IgG-HRP (1:2000; Cell Signaling Technology).

Zeta potential measurement
The sEV samples were resuspended in distilled water and loaded into disposable folded capillary cells. The zeta potential was measured using Zetasizer Nano ZS (Malvern Instruments).

TEM observation
sEV samples were fixed with 4% paraformaldehyde and layered on a carbon/Formvar film-coated TEM grid (Okenshoji Co., Ltd.) for 20 min at room temperature. After washing with PBS, the samples were treated with 1% glutaraldehyde for 5 min and washed four times with distilled water. Finally, they were stained with 1% uranyl acetate for 2 min. Observations were performed using a transmission electron microscope (JEOL, JEM-1400 Flash).

***In vitro* cellular uptake assay**
Peritoneal macrophages were incubated with 10 mg/mL of PKH67-labeled untreated or glycosidase-treated sEVs for 4 h at 37℃. The cells were washed twice with PBS and harvested. The cellular uptake of PKH67-labeled sEVs was determined by measuring the mean fluorescence intensity (MFI) using Gallios Flow Cytometer (Beckman Coulter, Miami, FL, USA) according to the manufacturer's instructions. Data were analyzed using the Kaluza software (version 1.0, Beckman Coulter). Because the degree of fluorescence labeling was not uniform between each sEV groups, the MFIs were corrected by the fluorescence intensity of the sEVs.

Pharmacokinetic analysis
The clearance of Gag-gLuc-labeled untreated and glycosidase-treated sEVs from the blood circulation upon tail-vein intravenous administration was measured based on luciferase activity, as described in previous sections. Time-course data were analyzed using noncompartmental analysis. The area under the curve (AUC), mean residence time (MRT), and clearance (CL) were calculated for each animal by integration from 5 to 120 min.

Statistical analysis
Differences among data sets were statistically analyzed by Student's t-test for paired comparisons and by Tukey-Kramer test for multiple comparisons. Values were considered statistically significant at $p < 0.05$.

III-3 Results

III-3-a Determination of glycosidase treatment condition using fetuin

To determine the amount of glycosidases used for sEV deglycosylation, fetuin was digested with varying doses of PNGaseF, O-glycosidase with neuraminidase, or a combination of the three glycosidases. CBB staining confirmed digestion of both N- and O-glycans from fetuin at the lowest dose for each glycosidase, which was indicated by a shift in the band due to a decrease in the molecular weight from the release of glycans after the enzyme treatment (Fig 17). Considering the structural differences between fetuin (soluble glycoprotein) and sEV membrane-bound glycoproteins, a medium dose of the glycosidase enzyme was selected for subsequent sEV isolation to ensure proper glycan digestion at the sEV surface.

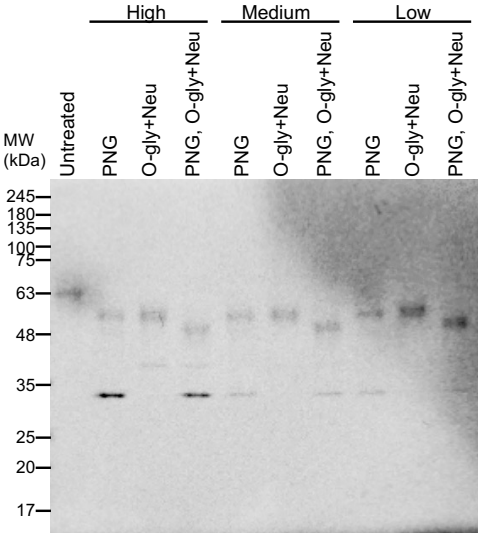

Figure 17.CBB staining of fetuin. Fetuin was incubated with low, medium, or high doses of PNGase F, O-glycosidase with neuraminidase, or a combination of the three glycosidases and incubated at 37°C for 3 h. PNG: PNGase F, O-gly: O-glycosidase, Neu: Neuraminidase

III-3-b Effect of deglycosylation on sEV physicochemical properties

Lectin blot analysis was performed to confirm the deglycosylation of sEV surface glycans at the determined dose. The specific lectins utilized, and its primary recognition sugars are listed in Table 2. Decreased molecular weight or staining intensity was observed in glycosidase-treated sEVs to varying degrees, depending on the lectin analyzed, confirming the successful removal of glycans by the enzyme treatment (Fig 18). Western blot analysis confirmed the presence of sEV marker proteins Alix, Hsp70, and CD81 in both untreated and glycosidase-treated sEVs. Additionally, Calnexin, and endoplasmic reticulum marker, was absent in all sEV groups, confirming negligible contamination from cell-derived debris in the collected sEV samples (Fig 19A). The physicochemical properties of the collected sEVs were evaluated based on zeta potential measurements and TEM observations. No significant differences in zeta potential were observed between untreated and glycosidase-treated sEVs (Fig 19B). Furthermore, TEM images revealed similar morphology and size distribution profiles for all sEV groups (Fig 19C), suggesting that glycosidase treatment did not significantly alter the physicochemical properties of sEVs.

Table 2. List of Lectins Utilized for detection of sEV glycosylation

Lectin	Origin	Primary recognition sugars
ConA	*Canavalia ensiformis*	α-D-Man, α-D-glc
DBA	*Dolichos biflorus*	α -D-GalNAc
WGA	*Triticum vulgaris*	D-GlcNAc, Sialic acid
PNA	*Arachis hypogaea*	Gal-β(1-3)-GalNAc
UEA I	*Ulex europaeus*	α-Fuc

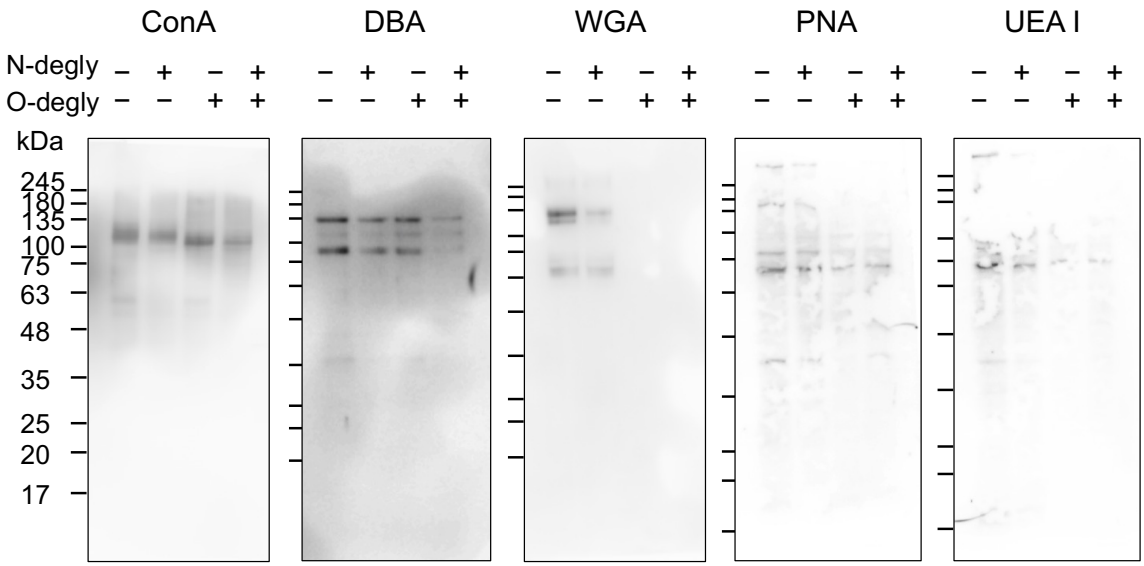

Figure 18. Glycosylation profile of glycosidase-treated sEVs. Lectin blotting for ConA, DBA, WGA, PNA, and UEA I in untreated and N-, O-, N+O-deglycosylated sEVs (0.5 μg protein/lane).

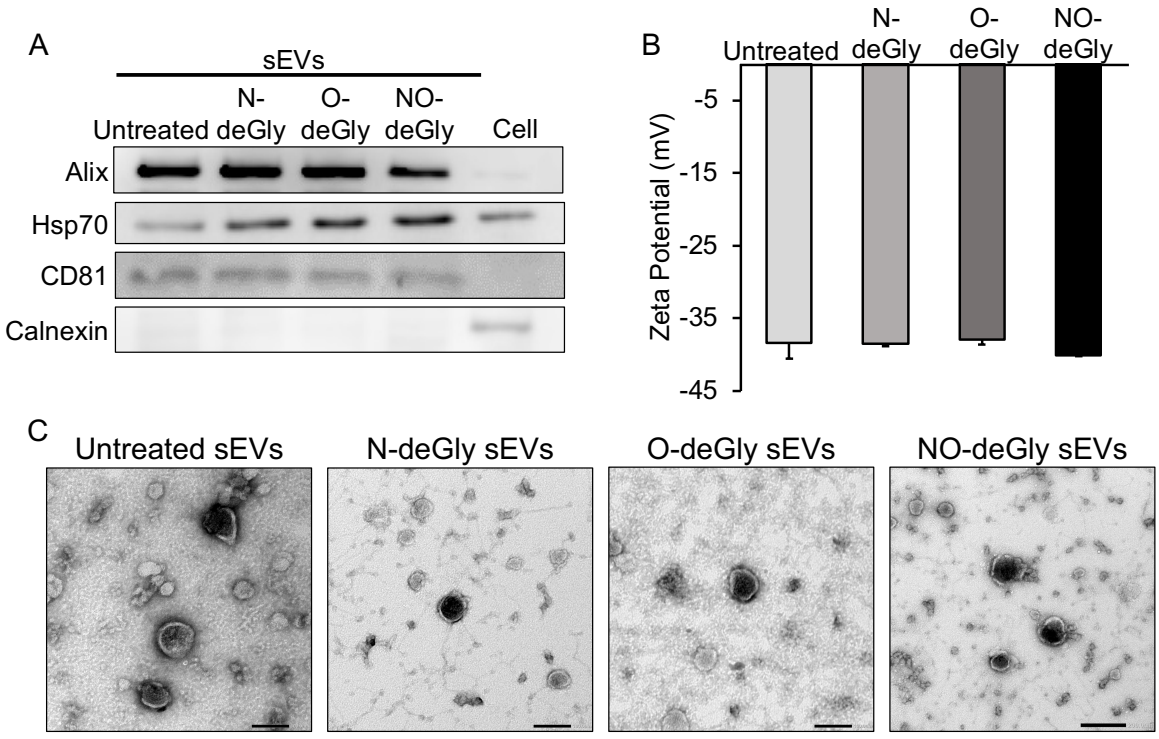

Figure 19. Effect of glycosidase treatment on sEV physicochemical properties. (a) Western blotting for Alix, Hsp70, CD81, and Calnexin in untreated and N-, O-, or N+O-deglycosylated sEVs and B16-BL6 cell lysates (0.5 μg protein/lane). (b) Zeta potential of untreated and N-, O-, or N+O-deglycosylated sEVs. Results are expressed as the mean ± standard deviation (n=3). (c) Transmission electron microscopy (TEM) images (scale bar = 100 nm). N-deGly: N-deglycosylated, O-deGly: O-deglycosylated, NO-deGly: N+O-deglycosylated.

III-3-c Effect of deglycosylation on sEV cellular uptake

Because macrophages in the liver and spleen significantly contribute to the clearance of systematically administered sEVs, the effect of glycosidase treatment on sEV uptake by peritoneal macrophages was evaluated. Glycosidase treatment that removes N-glycans as well as both N- and O-glycans significantly increased sEV uptake by peritoneal macrophages compared to that of the untreated sEVs. However, no significant differences in MFIs were observed in cells treated with O-glycosidase with neuraminidase and untreated sEVs (Fig 20).

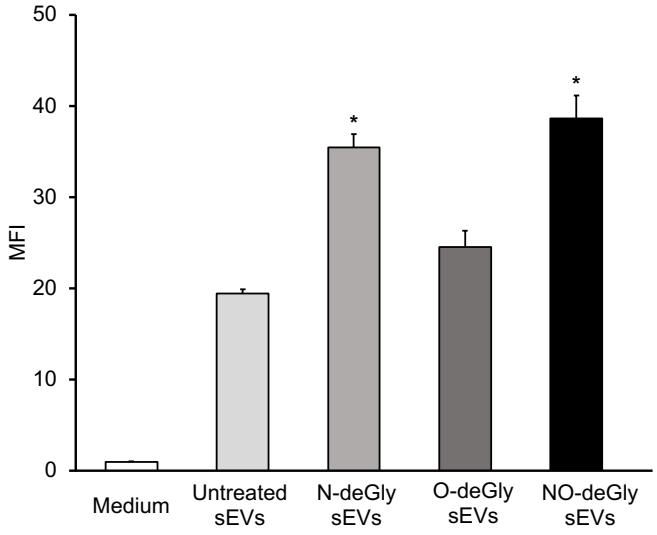

Figure 20. Cellular uptake of sEVs by peritoneal macrophages. Peritoneal macrophages were treated with PKH67-labeled untreated and N-, O-, or N+O-deglycosylated sEVs. After a 4 h incubation period, the MFI of the cells were measured using fluorescence-activated cell sorting to evaluate the cellular uptake of sEVs. The measured MFIs were corrected by the fluorescence intensity of the sEVs. Results are expressed as the mean ± standard deviation (n=3). N-deGly: N-deglycosylated, O-deGly: O-deglycosylated, NO-deGly: N+O-deglycosylated.

III-3-d Effect of deglycosylation on sEV pharmacokinetic

To evaluate the role of surface glycans in sEV pharmacokinetics, Gag-gLuc-labeled, glycosidase-treated sEVs were intravenously administered to mice. Both untreated and glycosidase-treated sEVs immediately disappeared from the blood circulation (Fig 21), and the pharmacokinetic parameters of the glycosidase-treated sEVs were comparable to those of the untreated sEVs, as shown in Table 3.

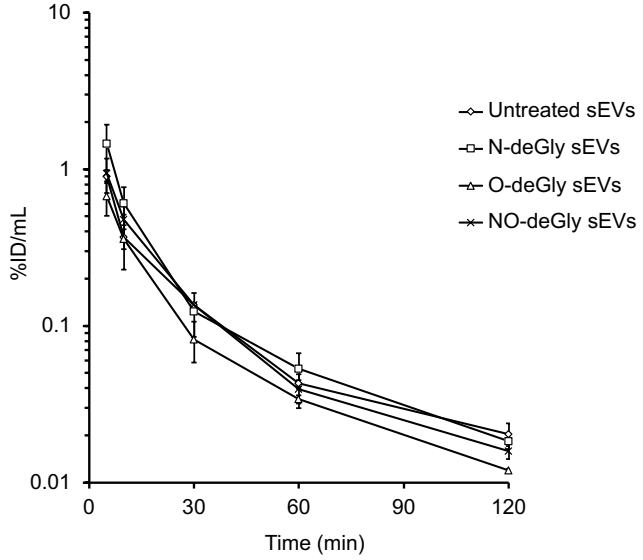

Figure 21. Evaluation of glycosidase-treated sEV clearance from the systemic circulation. Untreated and N-, O-, or N+O-deglycosylated sEVs were administered intravenously into the tail vein of mice. Serum gLuc activity was measured at indicated time points. The results are expressed as the mean ± standard deviation (n=3). N-deGly: N-deglycosylated, O-deGly: O-deglycosylated, NO-deGly: N+O-deglycosylated.

Table 3. PK analysis of intravenously injected sEVs

Sample	AUC (%ID·h/mL)	MRT (h)	CL (mL/h)
Untreated sEVs	0.234 ± 0.044	0.308 ± 0.021	438 ± 86
N-deGly sEVs	0.28 0± 0.094	0.285 ± 0.042	382 ± 108
O-deGly sEVs	0.181 ± 0.029	0.305 ± 0.033	564 ± 95
N+O-deGly sEVs	0.248 ± 0.048	0.295 ± 0.017	413 ± 72

Results are expressed as the mean ± standard deviation (n=3).

III-4 Discussion

The study of glycans in sEV research has lagged behind that of other major biomolecules such as membrane lipids and proteins, mainly due to the complexity of glycome analyses; however, there is growing awareness on the importance of glycans in sEV biology. Since glycans are located on the outermost region of sEV surface, it can be expected that surface glycans participate in various sEV functions, which ultimately influence their behavior in the body. Additionally, one of the hallmarks of cancer is alterations in glycosylation pattern, which could also be reflected in the sEV surface as well and influence disease progression. Thus, understanding the surface glycans of sEVs is crucial in furthering our knowledge on sEV biology.

In this study, fetuin-a glycoprotein commonly used as a positive control for glycosidase enzymes—was utilized to determine the deglycosylation treatment conditions for sEVs. The sEVs were then treated with glycosidase enzymes and washed twice with PBS via ultracentrifugation to eliminate residual enzymes in the sample. Deglycosylation of the sEVs were confirmed by lectin blot analysis. Removal of either N- or O-glycan resulted in a reduction in molecular weight or band intensity, and further reductions were observed in sEVs that had both glycans removed. This suggests the successful release of glycans from the sEV surface by the enzyme treatment. CBB staining of the isolated sEV did not show significant differences in their protein profiles (data not shown), suggesting that protein staining is not a suitable method for detecting sEV deglycosylation.

Glycosidase treatment affects sEV surface dynamics via the removal of glycans, and this could potentially change the physicochemical properties of sEVs, such as diameter and zeta potential[55]. However, results from this study showed that glycosidase treatment had little effect on the particle size and zeta potential of sEVs. This was contrary to previous reports that showed an increase in zeta potential upon deglycosylation—by treatment with neuraminidase and to a lesser extent, PNGase F—which was suggested to have resulted from the removal of sialic acid residues[56]. Indeed, the presence of large amounts of sialic acid residues contributing to the negative charge of cancer cell-derived sEVs have been previously reported[57]. Nonetheless, as demonstrated in our previous study, even the digestion of surface proteins through ProK treatment had little impact on sEV zeta potential[53]. Therefore, it can be surmised that surface proteins and glycans have little impact on the zeta potential of sEVs, and that the negative charge is likely derived from membrane lipids such as PS—a negatively charged phospholipid that is neither affected by ProK nor glycosidase treatment.

Further, removal of N-glycans significantly increased sEV uptake by macrophages; however, removal of O-glycans had minimal impact on sEV uptake. This was contrary to previous findings by Nishida-Aoki *et al*, where enhanced sEV uptake by the endothelial cells were observed for both N-glycan and O-glycan removed sEVs[49]. However, these differences could be attributed to the different type of cells utilized for the recipient and sEV producing cells. The increased uptake observed by the removal of N-glycans in melanoma cell derived sEVs suggest an inhibitory role of N-glycans in the cellular uptake of sEVs by the macrophages. Since PNGase F removes almost all N-glycans from the sEV surface, it is possible that this decreased the steric hindrance of other surface ligands, which allowed for better access to cell surface receptors for cellular uptake.

However, despite the increased uptake by macrophages observed *in vitro*, the pharmacokinetic profiles of PNGase F-treated sEVs were comparable to those of untreated sEVs *in vivo*. This implies that the increased uptake efficiency of macrophages did not increase the clearance rate of the sEVs from the blood circulation. This is probably due to macrophages intrinsically having a significantly high sEV clearance capability, such that the rate determining process in sEV clearance in the liver is blood-flow rate-dependent and not on the sEV uptake capacity of the macrophages. Hepatic clearance—defined as the volume of blood perfusing the liver that is cleared of drug (in this case, sEVs) per unit of time—is determined by the following three parameters: 1) blood flow through the liver, 2) fraction of unbound drug in the blood, and 3) intrinsic capability of hepatic enzymes to metabolize the drug[58]. Drugs with high intrinsic capacity are efficiently cleared from the liver, and its hepatic clearance is limited by the hepatic blood-flow rate. Contrastingly, drugs with low intrinsic capacity have a hepatic clearance that is dependent on the fraction of unbound drug and its metabolizing capacity in the liver. Previously, we have reported that macrophages play an important role in the clearance of sEVs from the blood circulation upon intravenous administration. In that study, we found that the macrophage-depleted mice decreased the sEV clearance to 1.6% of that in control mice, which indicates that macrophages have a significantly high intrinsic capability to clear the sEVs from the blood circulation[59]. This, along with the fact that sEV clearance did not change despite differences in cellular uptake upon glycosidase treatment *in vitro* strongly supports our hypothesis that sEVs have a blood-flow rate-dependent hepatic clearance. Nevertheless, further pharmacokinetic studies using mice with altered blood flow (either by manipulation of environmental temperature or utilizing disease models that are known to have decreased blood flow) or decreased intrinsic clearance (by manipulation of the number of residing macrophages in the liver) are necessary to confirm this hypothesis. Regardless, these results support our previous hypothesis that PS is the major component recognized by macrophages that contributes to sEV clearance at the whole-body level.

Summary

Development of a sensitive sEV quantification method is integral to sEV research. Considering the limitations of the current sEV quantification methods that is observed in literature, I aimed to develop a sEV quantification assay that is both robust and sensitive to further our understanding of sEV production and *in vivo* fates in the body. The main findings from each chapter are summarized as follows.

Chapter I Development of a highly sensitive sEV quantification method and the identification of novel sEV modulators via high throughput screening
sEV quantification method based on luciferase enzyme was developed by fusing gLuc reporter protein with sEV marker protein, CD63. This method allowed for high throughput quantification of sEVs with minimal purification steps. Using the developed quantification method, total of 480 compounds were screened, and two compounds were identified to modulate sEV production—KPYC08425 and KPYC12163. Although the mechanism remains unclear, KPYC08425 improved sEV protein yield by 1.5-folds. Contrastingly, KPYC12163 showed significant reduction in sEV protein yield by approximately 70%, likely by inhibiting its release and inducing autophagy-lysosomal pathway.

Chapter II Pharmacokinetic approach for the elucidation of elevated plasma sEV concentration during cancer pathogenesis
Using the gLuc fusion protein, the *in vivo* fates of sEVs during cancer pathogenesis was evaluated. Plasma sEV levels are known to increase significantly during cancer, and increased sEV protein yield was confirmed in B16BL6 tumor-bearing mice models. By labeling the MP-sEVs isolated from healthy and tumor-bearing mice with gLuc-LA fusion protein, the sEV clearance rates in both healthy and tumor-bearing mice were determined. Results showed that the sEV clearance rate is unaltered in cancer. Therefore, it was presumed that the increased sEV production rate was the main driving force for the increased plasma sEV levels. Further analysis showed that tumor cell-derived sEVs contributed very little the overall MP-sEV protein yield, thereby suggesting cells other than tumor cells mainly contributed to the increased MP-sEV observed during cancer.

Chapter III Determination of the effect of surface glycans in sEV pharmacokinetics
Continuing from chapter II, the *in vivo* fates of sEVs pre-treated with glycosidase enzymes were evaluated to determine the effect of surface glycans on sEV pharmacokinetics. Surface glycans play a significant role in sEV function, and based on its location, could impact its pharmacokinetics. Deglycosylation of surface glycans on the sEV membrane utilizing PNGase F and O-glycosidase was confirmed by lectin blot analysis. Deglycosylation treatment hardly altered the sEV physicochemical properties, however the removal of N-glycans increased the uptake of sEVs by the peritoneal macrophages. Regardless, sEV pharmacokinetics were unaltered by the deglycosylation treatment, suggesting that the increased uptake efficiency by the macrophages observed *in vitro* did not increase the clearance rate of the sEVs *in vivo*. This was likely due to the intrinsically high sEV clearance capability of the macrophages, which then suggests that the rate-determining process in sEV clearance is likely blood-flow rate-dependent, and not on the sEV uptake capacity of the macrophages.

The findings in this thesis contribute to our understanding on the biological and pathological roles of sEVs and to the development of sEV-based therapies.

Acknowledgements

First and foremost, I would like to express my deepest appreciation to my advisor, Professor Yoshinobu Takakura, Ph.D. from the Department of Biopharmaceutics and Drug Metabolism, Graduate School of Pharmaceutical Sciences, Kyoto University for graciously welcoming me into his laboratory and giving me the opportunity to study under his guidance. His encouragements and advice truly supported my years as a doctorate student here at Kyoto University.

I would also like to extend my deepest gratitude to Associate Professor Yuki Takahashi, Ph.D. from the Department of Biopharmaceutics and Drug Metabolism. His passion for research has inspired many students including myself, and his extensive knowledge, constructive criticism, and unwavering guidance truly assisted me in completing my thesis. I could not have asked for a better advisor for my Ph.D. study besides Dr. Takakura and Dr. Takahashi, and to that I am sincerely grateful for.

I would also like to extend my sincere thanks to Associate Professor Shinsuke Inuki, Ph.D. and Professor Hiroaki Ohno, Ph.D. from the Department of Bioorganic Medicinal Chemistry and Chemogenomics for the compound libraries, and Professor Masao Doi, Ph.D. from the Department of System Biology and his laboratory member, Mr. Shumepi Nakagawa, MS for their assistance in the screening in Chapter I. Additionally, I would also like to thank Ms. Keiko Okamoto-Furuta and Mr. Haruyasu Kohda from the Division of Electron Microscopic Study, Center for Anatomical Studies, Graduate School of Medicines, Kyoto University for their technical assistance in electron microscopy studies in Chapter I.

Many thanks to my mentor, Dr. Takuma Yamashita and Dr. Akihiro Matsumoto for their valuable input, suggestions, and fruitful discussions. Additionally, I would like to thank both the alumni and residing members of the Department of Biopharmaceutics and Drug Metabolism for their experimental assistances as well as the great memories we have shared over the past four years. I would like to give my special thanks to Ms. Yukari Yasue, Mr. Asahi Yoshida, and Ms. Mihiro Toba for their unstinting assistances.

Last but not least, I would like to thank my friends and family who have supported me through all the ups and downs during this long journey of my Ph.D. study. Thank you to Dr. Austin Ferrara and Dr. Myroslava Sharabun for their relentless support and words of encouragement; you were always there when I needed you, even though I was halfway across the world. Thank you to my two brothers for their unparalleled support and care, especially after the coronavirus pandemic. A deep thank you to my mother for her continuous and unwavering love, help, and support from the very first step of this journey. And lastly, I would like to give my sincere thanks to my hero, my father. You introduced me to the world of pharmaceutics and you taught me the joy of science and scientific research. Thank you for letting me chase my dreams, and providing me all the opportunities and experiences that have made me who I am today.

References

1. Lässer C, Seyed Alikhani V, Ekström K, et al. Human saliva, plasma and breast milk exosomes contain RNA: uptake by macrophages. *Journal of Translational Medicine*. 2011;9(1). doi:10.1186/1479-5876-9-9
2. Fujita K, Nonomura N. Urinary biomarkers of prostate cancer. *International Journal of Urology*. 2018;25(9). doi:10.1111/iju.13734
3. el Andaloussi S, Mäger I, Breakefield XO, Wood MJA. Extracellular vesicles: biology and emerging therapeutic opportunities. *Nature Reviews Drug Discovery*. 2013;12(5). doi:10.1038/nrd3978
4. Zaborowski MP, Balaj L, Breakefield XO, Lai CP. Extracellular Vesicles: Composition, Biological Relevance, and Methods of Study. *BioScience*. 2015;65(8). doi:10.1093/biosci/biv084
5. van Niel G, D'Angelo G, Raposo G. Shedding light on the cell biology of extracellular vesicles. *Nature Reviews Molecular Cell Biology*. 2018;19(4). doi:10.1038/nrm.2017.125
6. Hartjes T, Mytnyk S, Jenster G, van Steijn V, van Royen M. Extracellular Vesicle Quantification and Characterization: Common Methods and Emerging Approaches. *Bioengineering*. 2019;6(1). doi:10.3390/bioengineering6010007
7. Cloet T, Momenbeitollahi N, Li H. Recent advances on protein-based quantification of extracellular vesicles. *Analytical Biochemistry*. 2021;622. doi:10.1016/j.ab.2021.114168
8. Maas SLN, Broekman MLD, de Vrij J. Tunable Resistive Pulse Sensing for the Characterization of Extracellular Vesicles. In: ; 2017. doi:10.1007/978-1-4939-6728-5_2
9. Yoshioka Y, Kosaka N, Konishi Y, et al. Ultra-sensitive liquid biopsy of circulating extracellular vesicles using ExoScreen. *Nature Communications*. 2014;5(1). doi:10.1038/ncomms4591
10. Ueda K, Ishikawa N, Tatsuguchi A, Saichi N, Fujii R, Nakagawa H. Antibody-coupled monolithic silica microtips for highthroughput molecular profiling of circulating exosomes. *Scientific Reports*. 2015;4(1). doi:10.1038/srep06232
11. Shen W, Guo K, Adkins GB, et al. A Single Extracellular Vesicle (EV) Flow Cytometry Approach to Reveal EV Heterogeneity. *Angewandte Chemie International Edition*. 2018;57(48). doi:10.1002/anie.201806901
12. Nakai W, Yoshida T, Diez D, et al. A novel affinity-based method for the isolation of highly purified extracellular vesicles. *Scientific Reports*. 2016;6(1). doi:10.1038/srep33935
13. Taylor DD, Shah S. Methods of isolating extracellular vesicles impact down-stream analyses of their cargoes. *Methods*. 2015;87. doi:10.1016/j.ymeth.2015.02.019
14. Yáñez-Mó M, Siljander PR-M, Andreu Z, et al. Biological properties of extracellular vesicles and their physiological functions. *Journal of Extracellular Vesicles*. 2015;4(1). doi:10.3402/jev.v4.27066
15. Tkach M, Théry C. Communication by Extracellular Vesicles: Where We Are and Where We Need to Go. *Cell*. 2016;164(6). doi:10.1016/j.cell.2016.01.043
16. Becker A, Thakur BK, Weiss JM, Kim HS, Peinado H, Lyden D. Extracellular Vesicles in Cancer: Cell-to-Cell Mediators of Metastasis. *Cancer Cell*. 2016;30(6). doi:10.1016/j.ccell.2016.10.009
17. Catalano M, O'Driscoll L. Inhibiting extracellular vesicles formation and release: a review of EV inhibitors. *Journal of Extracellular Vesicles*. 2020;9(1). doi:10.1080/20013078.2019.1703244
18. Khan FM, Saleh E, Alawadhi H, Harati R, Zimmermann W-H, El-Awady R. Inhibition of exosome release by ketotifen enhances sensitivity of cancer cells to doxorubicin. *Cancer Biology & Therapy*. 2018;19(1). doi:10.1080/15384047.2017.1394544
19. Kulshreshtha A, Singh S, Ahmad M, et al. Simvastatin mediates inhibition of exosome synthesis, localization and secretion via multicomponent interventions. *Scientific Reports*. 2019;9(1). doi:10.1038/s41598-019-52765-7
20. Ludwig N, Yerneni SS, Menshikova E v., Gillespie DG, Jackson EK, Whiteside TL. Simultaneous Inhibition of Glycolysis and Oxidative Phosphorylation Triggers a Multi-Fold Increase in Secretion of Exosomes: Possible Role of 2′,3′-cAMP. *Scientific Reports*. 2020;10(1). doi:10.1038/s41598-020-63658-5
21. Emam SE, Ando H, Abu Lila AS, et al. A Novel Strategy to Increase the Yield of Exosomes (Extracellular Vesicles) for an Expansion of Basic Research. *Biological and Pharmaceutical Bulletin*. 2018;41(5). doi:10.1248/bpb.b17-00919
22. García-Seisdedos D, Babiy B, Lerma M, et al. Curcumin stimulates exosome/microvesicle release in an in vitro model of intracellular lipid accumulation by increasing ceramide synthesis. *Biochimica et Biophysica Acta (BBA) - Molecular and Cell Biology of Lipids*. 2020;1865(5). doi:10.1016/j.bbalip.2020.158638
23. Im E-J, Lee C-H, Moon P-G, et al. Sulfisoxazole inhibits the secretion of small extracellular vesicles by targeting the endothelin receptor A. *Nature Communications*. 2019;10(1). doi:10.1038/s41467-019-09387-4
24. Datta A, Kim H, McGee L, et al. High-throughput screening identified selective inhibitors of exosome biogenesis and secretion: A drug repurposing strategy for advanced cancer. *Scientific Reports*. 2018;8(1).

doi:10.1038/s41598-018-26411-7
25. Logozzi M, de Milito A, Lugini L, et al. High Levels of Exosomes Expressing CD63 and Caveolin-1 in Plasma of Melanoma Patients. *PLoS ONE*. 2009;4(4). doi:10.1371/journal.pone.0005219
26. Peinado H, Alečković M, Lavotshkin S, et al. Melanoma exosomes educate bone marrow progenitor cells toward a pro-metastatic phenotype through MET. *Nature Medicine*. 2012;18(6). doi:10.1038/nm.2753
27. Theodoraki M-N, Matsumoto A, Beccard I, Hoffmann TK, Whiteside TL. CD44v3 protein-carrying tumor-derived exosomes in HNSCC patients' plasma as potential noninvasive biomarkers of disease activity. *OncoImmunology*. 2020;9(1). doi:10.1080/2162402X.2020.1747732
28. Rodríguez Zorrilla S, Pérez-Sayans M, Fais S, Logozzi M, Gallas Torreira M, García García A. A Pilot Clinical Study on the Prognostic Relevance of Plasmatic Exosomes Levels in Oral Squamous Cell Carcinoma Patients. *Cancers*. 2019;11(3). doi:10.3390/cancers11030429
29. Cappello F, Logozzi M, Campanella C, et al. Exosome levels in human body fluids: A tumor marker by themselves? *European Journal of Pharmaceutical Sciences*. 2017;96. doi:10.1016/j.ejps.2016.09.010
30. Nishida-Aoki N, Tominaga N, Takeshita F, Sonoda H, Yoshioka Y, Ochiya T. Disruption of Circulating Extracellular Vesicles as a Novel Therapeutic Strategy against Cancer Metastasis. *Molecular Therapy*. 2017;25(1). doi:10.1016/j.ymthe.2016.10.009
31. Marleau AM, Chen C-S, Joyce JA, Tullis RH. Exosome removal as a therapeutic adjuvant in cancer. *Journal of Translational Medicine*. 2012;10(1). doi:10.1186/1479-5876-10-134
32. Gupta D, Liang X, Pavlova S, et al. Quantification of extracellular vesicles in vitro and in vivo using sensitive bioluminescence imaging. *Journal of Extracellular Vesicles*. 2020;9(1). doi:10.1080/20013078.2020.1800222
33. Verweij FJ, Bebelman MP, Jimenez CR, et al. Quantifying exosome secretion from single cells reveals a modulatory role for GPCR signaling. *Journal of Cell Biology*. 2018;217(3). doi:10.1083/jcb.201703206
34. Hikita T, Miyata M, Watanabe R, Oneyama C. Sensitive and rapid quantification of exosomes by fusing luciferase to exosome marker proteins. *Scientific Reports*. 2018;8(1). doi:10.1038/s41598-018-32535-7
35. McCann J v., Bischoff SR, Zhang Y, et al. Reporter mice for isolating and auditing cell type-specific extracellular vesicles in vivo. *Genesis*. 2020;58(7). doi:10.1002/dvg.23369
36. Luo W, Dai Y, Chen Z, Yue X, Andrade-Powell KC, Chang J. Spatial and temporal tracking of cardiac exosomes in mouse using a nano-luciferase-CD63 fusion protein. *Communications Biology*. 2020;3(1). doi:10.1038/s42003-020-0830-7
37. Neckles VN, Morton MC, Holmberg JC, et al. A transgenic inducible GFP extracellular-vesicle reporter (TIGER) mouse illuminates neonatal cortical astrocytes as a source of immunomodulatory extracellular vesicles. *Scientific Reports*. 2019;9(1). doi:10.1038/s41598-019-39679-0
38. Matsumoto A, Takahashi Y, Chang H, et al. Blood concentrations of small extracellular vesicles are determined by a balance between abundant secretion and rapid clearance. *Journal of Extracellular Vesicles*. 2020;9(1). doi:10.1080/20013078.2019.1696517
39. Liang Y, Eng WS, Colquhoun DR, Dinglasan RR, Graham DR, Mahal LK. Complex N-linked glycans serve as a determinant for exosome/microvesicle cargo recruitment. *Journal of Biological Chemistry*. 2014;289(47). doi:10.1074/jbc.M114.606269
40. Gomes J, Gomes-Alves P, Carvalho S, et al. Extracellular Vesicles from Ovarian Carcinoma Cells Display Specific Glycosignatures. *Biomolecules*. 2015;5(3). doi:10.3390/biom5031741
41. Christianson HC, Svensson KJ, van Kuppevelt TH, Li J-P, Belting M. Cancer cell exosomes depend on cell-surface heparan sulfate proteoglycans for their internalization and functional activity. *Proceedings of the National Academy of Sciences*. 2013;110(43). doi:10.1073/pnas.1304266110
42. Costa J. Glycoconjugates from extracellular vesicles: Structures, functions and emerging potential as cancer biomarkers. *Biochimica et Biophysica Acta - Reviews on Cancer*. 2017;1868(1):157-166. doi:10.1016/j.bbcan.2017.03.007
43. Escrevente C, Keller S, Altevogt P, Costa J. Interaction and uptake of exosomes by ovarian cancer cells. *BMC Cancer*. 2011;11(1). doi:10.1186/1471-2407-11-108
44. Williams C, Royo F, Aizpurua-Olaizola O, et al. Glycosylation of extracellular vesicles: current knowledge, tools and clinical perspectives. *Journal of Extracellular Vesicles*. 2018;7(1). doi:10.1080/20013078.2018.1442985
45. Gerlach JQ, Griffin MD. Getting to know the extracellular vesicle glycome. *Molecular BioSystems*. 2016;12(4). doi:10.1039/C5MB00835B
46. Iwao Y, Hiraike M, Kragh-Hansen U, et al. Altered chain-length and glycosylation modify the pharmacokinetics of human serum albumin. *Biochimica et Biophysica Acta - Proteins and Proteomics*. 2009;1794(4):634-641. doi:10.1016/j.bbapap.2008.11.022
47. Brzezicka K, Vogel U, Serna S, Johannssen T, Lepenies B, Reichardt N-C. Influence of Core β-1,2-Xylosylation on Glycoprotein Recognition by Murine C-type Lectin Receptors and Its Impact on Dendritic Cell Targeting. *ACS Chemical Biology*. 2016;11(8). doi:10.1021/acschembio.6b00265
48. Frenz T, Grabski E, Durán V, et al. Antigen presenting cell-selective drug delivery by glycan-decorated nanocarriers. *European Journal of Pharmaceutics and Biopharmaceutics*. 2015;95. doi:10.1016/j.ejpb.2015.02.008

49. Nishida-Aoki N, Tominaga N, Kosaka N, Ochiya T. Altered biodistribution of deglycosylated extracellular vesicles through enhanced cellular uptake. *Journal of Extracellular Vesicles*. 2020;9(1). doi:10.1080/20013078.2020.1713527
50. Royo F, Cossío U, Ruiz De Angulo A, Llop J, Falcon-Perez JM. Modification of the glycosylation of extracellular vesicles alters their biodistribution in mice. *Nanoscale*. 2019;11(4):1531-1537. doi:10.1039/c8nr03900c
51. Freeze HH, Kranz C. Endoglycosidase and Glycoamidase Release of N-Linked Glycans. *Current Protocols in Molecular Biology*. 2010;89(1). doi:10.1002/0471142727.mb1713as89
52. Yoshida H, Nishikawa M, Yasuda S, Mizuno Y, Takakura Y. Cellular activation by plasmid dna in various macrophages in primary culture. *Journal of Pharmaceutical Sciences*. 2008;97(10). doi:10.1002/jps.21302
53. Charoenviriyakul C, Takahashi Y, Morishita M, Nishikawa M, Takakura Y. Role of Extracellular Vesicle Surface Proteins in the Pharmacokinetics of Extracellular Vesicles. *Molecular Pharmaceutics*. 2018;15(3). doi:10.1021/acs.molpharmaceut.7b00950
54. Takahashi Y, Nishikawa M, Shinotsuka H, et al. Visualization and in vivo tracking of the exosomes of murine melanoma B16-BL6 cells in mice after intravenous injection. *Journal of Biotechnology*. 2013;165(2). doi:10.1016/j.jbiotec.2013.03.013
55. Fernandes HP, Cesar CL, Barjas-Castro M de L. Electrical properties of the red blood cell membrane and immunohematological investigation. *Revista Brasileira de Hematologia e Hemoterapia*. 2011;33(4). doi:10.5581/1516-8484.20110080
56. Williams C, Pazos R, Royo F, et al. Assessing the role of surface glycans of extracellular vesicles on cellular uptake. *Scientific Reports*. 2019;9(1). doi:10.1038/s41598-019-48499-1
57. Akagi T, Kato K, Hanamura N, Kobayashi M, Ichiki T. Evaluation of desialylation effect on zeta potential of extracellular vesicles secreted from human prostate cancer cells by on-chip microcapillary electrophoresis. *Japanese Journal of Applied Physics*. 2014;53(6S). doi:10.7567/JJAP.53.06JL01
58. Laveé T, Funk C. In Vivo Absorption, Distribution, Metabolism, and Excretion Studies in Discovery and Development. In: *Comprehensive Medicinal Chemistry II*. Elsevier; 2007. doi:10.1016/B0-08-045044-X/00118-8
59. Imai T, Takahashi Y, Nishikawa M, et al. Macrophage-dependent clearance of systemically administered B16BL6-derived exosomes from the blood circulation in mice. *Journal of Extracellular Vesicles*. 2015;4(2015):1-8. doi:10.3402/jev.v4.26238